

Microscopic and thermodynamic evaluation of vesicles shed by erythrocytes at elevated temperatures.

T. Moore^a, I. Sorokulova^a, O. Pustovyy^a, L. Globa^a, D. Pascoe^b, M. Rudisill^b and Vitaly Vodyanoy^{a*}

^a College of Veterinary Medicine, Auburn University, Auburn AL 36849; ^b College of Education, Auburn University, Auburn AL 36849

(Dated: February 2, 2013)

Erythrocytes and vesicles shed by erythrocytes from human and rat blood were collected and analyzed after temperature was elevated by physical exercise or by exposure to external heat. The images of erythrocytes and vesicles were analyzed by the light microscopy system with spatial resolution of better than 90 nm. The samples were observed in an aqueous environment and required no freezing, dehydration, staining, shadowing, marking or any other manipulation. Temperature elevation, whether passive or through exercise, resulted in significant concentration increase of structurally transformed erythrocytes (echinocytes) and vesicles in blood. At temperature of 37 °C, mean vesicle concentrations and diameters in human and rat blood were $(1.50 \pm 0.35) \times 10^6$ and $(1.4 \pm 0.2) \times 10^6$ vesicles/ μ L, and 0.365 ± 0.065 and 0.436 ± 0.03 μ m, respectively. It was estimated that 80% of all vesicles found in human blood are smaller than 0.4 μ m. Thermodynamic analysis of experimental and literature data showed that erythrocyte transformation, vesicle release and other associated processes are driven by entropy with enthalpy-entropy compensation. It is suggested that physical state of hydrated cell membrane is responsible for the compensation. The increase of vesicle number related to elevated temperatures may be indicative of the heat stress level and serve as diagnostic of erythrocyte stability and human performance.

Key words: Erythrocytes, echinocytes, vesicles, entropy, microscopy, heat stress

1. Introduction

All organisms in order to maintain wellbeing must preserve a homeostasis, which is constantly affected by internal or external adverse forces termed stressors. Temperature represents one of the most challenging stressors. Although humans have the capability to withstand large variations in environmental temperatures, relatively small increases in internal temperature can lead to injury, heatstroke and even death (Crandall and Gonzalez-Alonso, 2010). Exposure to hot weather is considered one of the most deadly natural hazards in the United States. It was estimated that between 1979 and 2002, heatstroke claimed more American lives than the combined effects of hurricanes, lightning, earthquakes, floods, and tornadoes (Leon and Helwig, 2010).

Heat stress, whether passive (i.e. exposure to elevated environmental temperatures) or via the metabolic heat of exercise, results in pronounced cardiovascular adjustments that might involve the interplay of both local and central reflexes in humans (Crandall and Gonzalez-Alonso, 2010). Central and peripheral fatigue was found to be manifested in reduction of force production that was measured immediately after passive and exercise-Induced heat (Periard et al., 2011). These results agree well with those showing that an elevated

core temperature is the primary factor contributing to central fatigue during isometric contractions and hyperthermia (Morrison et al., 2004). Studies with rats have shown that body temperature elevation during exercise is important for induction of exercise-increased shock protein 72 level in rat plasma (Ogura et al., 2008).

Vesicles constitute a heterogenic population of cell-derived microscopic size particles that participate in a wide range of physiological and pathological processes. They derive from different cell types including platelets, red blood cells, leucocytes endothelial, smooth muscle, and cancer cells (Burnier et al., 2009; Castellana et al., 2010; Jayachandran et al., 2008; Orozco and Lewis, 2010; Roos et al., 2010; Rubin et al., 2008; VanWijk et al., 2003; Willekens et al., 1997; Willekens et al., 2003; Willekens et al., 2008; Willekens, 2010). In this work we concentrated on the vesicles in blood plasma, focusing on the red blood cell vesiculation (Greenwalt, 2006) at conditions of elevated temperatures (Araki et al., 1982; Baar, 1974; Bessis, 1972; Chernitskii et al., 1994; Christel and Little, 1984; Gershfeld and Murayama, 1988; Glaser, 1979; Ham et al., 1948; Ivanov et al., 2007; Leonards and Ohki, 1983; Loebel et al., 1973; Longster et al., 1972; Przybylska et al., 2000; Rubin et al., 2008; Samoylov et al., 2005;

Schultze, 1865; Wagner et al., 1986; Walsh and Whitham, 2006).

Mature erythrocytes undergo aging and eventually they are recognized and cleared by macrophages (Rous, 1923; Rous and Robertson, 1917). More recently, it was shown that the aging erythrocyte is characterized by changes in the plasma membrane, that make them selectively recognized by macrophages and then phagocytized in spleen, liver, or bone marrow (Ghashghaieina et al., 2012). This process is termed eryptosis or programmed erythrocyte death (Bratosin et al., 2001; Föller et al., 2008; Lang and Qadri, 2012; Vittori et al., 2012).

Eryptosis, is characterized by erythrocyte volume reduction, membrane vesiculation (release of small vesicles) and cell membrane phosphatidylserine externalisation. Phosphatidylserine-exposing erythrocytes are recognized by macrophages, which engulf and ingest the dying cells. The regulated form of eryptosis is induced by Ca^{2+} influx, and prevented by cysteine protease inhibitors (Bratosin et al., 2001). Prominent among known triggers of eryptosis (Bosman et al., 2011; Lang et al., 2010; Lutz et al., 1977; Richards et al., 2007) is hyperthermia (Foller et al., 2010).

An elevation in cytosolic Ca^{2+} activity, is known to initiate cell membrane vesiculation, cell membrane scrambling and activation of the cysteine endopeptidase calpain, an enzyme degrading the cytoskeleton and thus causing cell membrane blebbing or bulging. Ca^{2+} further stimulates Ca^{2+} -sensitive K^+ channels, the following outflow of K^+ hyperpolarizes the cell membrane, which causes outflow of Cl^- . The cellular loss of KCl with osmotically driven water leads to cell shrinkage and phosphatidylserine externalization of eryptotic cells. This leads to macrophage recognition and ingestion of dying erythrocytes (Lang and Qadri, 2012).

It has been demonstrated *in vitro* that the normal red blood cells (discocytes) go through shape changes at variation of temperature. The elevated temperature, induces a series of crenated shapes (echinocytes), characterized by convex rounded protrusions or spicules. Gradually, the spicules become smaller and more numerous and eventually bud off irreversibly, forming extracellular vesicles composed of plasma membrane materials (Christel and Little, 1984; Gedde and Huestis, 1997; Glaser, 1979; Glaser and Donath, 1992; Henszen et al., 1997; Muller et al., 1986). We hypothesize that elevation of temperature during a heat stress may cause transformation of some of the normal erythrocytes (discocytes) into speculated echinocytes that shed membrane vesicles. The increase of the

number of membrane vesicles produced during heat stress is relational to a number of discocyte-echinocyte transitions. Therefore, the increase of vesicle numbers following heat stress may be indicative of and proportional to the stress level.

2. Methods

2.1 Subjects and protocols

2.1.1 Human case study

One healthy male volunteer (age 61) was recruited. One week prior to beginning of heat protocol the volunteer was invited for assessment of maximal oxygen consumption ($\text{VO}_{2\text{max}}$) and anthropometric data (body weight, body composition, height, etc.). Once a week the volunteer exercised after overnight fast at euhydrated state on the treadmill at a work rate corresponding to 80% of the $\text{VO}_{2\text{max}}$. Exercise continued each day until core temperatures was elevated 1, 2, and 3°C above resting. Small blood samples (7 μL) were collected before and after exercise. The subject inserted a rectal thermometer 10cm past the anal sphincter for continual monitoring of core body temperature and places a heart rate (HR) on their chest for continual HR monitoring.

2.1.2 Animals

Adult Sprague-Dawley male rats weighing 250-300 g were used. The animals were housed two in a cage under standardized conditions of temperature ($20 \pm 1^{\circ}\text{C}$), humidity ($50 \pm 5\%$) and lighting (12-h day/12-h night) with free access to food and water. Two groups of rats (5 rats in control, and 4 rats in stress group) were studied. These groups are: 1) control (25°C) and 2) stress (45°C , 25 min). Animals from group 2 were exposed to 45°C heat stress, relative humidity 55% for 25 min in a 1610 Caron Environmental Chamber control animals (group 1) were exposed to identical conditions as the heat stressed animals, but at 25°C . Four hours after the stress experiments small samples (7 μL) of blood were taken from each rat for live cells and vesicles and examined with light microscopy. Temperature of each rat was measured with an infrared digital thermographic camera (Flir B360 High-Sensitivity Infrared Thermal Imaging Camera) placed 50 cm from the animal. This camera has a thermal sensitivity of approximately 0.1 $^{\circ}\text{C}$ and a spatial resolution of 320×240 pixels. The temperature was measured remotely inside the ear (Vianna and Carrive, 2005).

2.2 High resolution light microscopy of blood

The microscope system produces the highly oblique hollow cone of light (N.A. 1.2-1.4). Coupled with a high aperture microscope objective with iris, this system provides two different regimes of illumination. When the iris is closed so that no direct light enters the objective after passing through the object, only refracted, scattered, or diffracted light goes in the objective. If the iris is open in such a way to allow the direct entrance of light into objective the front lens of the objective is illuminated by the annular light produced by the empty cone of light entering the objective. In this case the mixed illumination is produced that combines the darkfield and oblique hollow cone brightfield illuminations. The cardioid condenser is an integral part of the illumination system so that the system comprises a collimation lenses and a first surface mirror that focus light onto the annular entrance slit of the condenser. As a part of the illumination system, the condenser is pre-aligned and therefore additional alignment is unnecessary. The illumination system is positioned in Olympus BX51 microscope by replacing a regular brightfield condenser. The illumination system is connected with a light source (EXFO120, Photonic Solution) by a liquid light guide. The objective used for this work is infinity corrected objective HCX PL APO 100×/1.40-0.70, oil, iris from Leica. The image is magnified with a zoom intermediate lens (2×-U-CA, Olympus), a homebuilt 40× relay lens, and captured by a Peltier-cooled camera (AxioCam HRc, Zeiss) and Dimension 8200 Dell computer. The microscope is placed onto a vibration isolation platform (TMS, Peabody, MA). Live images were recorded with Sony DXC-33 Video camera and Mac OS X Computer (Vainrub et al., 2006). Test images were calibrated using a Richardson slide (Richardson, 1988). A small droplet (7 μL) of freshly drawn blood were placed on a glass slide and coverslipped and positioned on the microscope stage with oil contacts between condenser and objective lenses. Ten image frames of $72 \times 53.3 \mu\text{m}^2$ in each sample were photographed, videotaped, and concentrations of discocytes, echinocytes, and vesicle count and diameter were measured by Image-Pro Plus software (Media Cybernetics), providing high-resolution direct-view optical images in real time. The samples were observed in an aqueous environment and required no freezing, dehydration, staining, shadowing, marking or any other manipulation. At least 20 image frames were analyzed for each experimental condition. Each frame contained at average between 50 and 200 vesicles (depending on conditions).

2.3 Thermodynamic calculations of the erythrocyte vesiculation

During a normal lifespan, an erythrocyte reduces its volume and surface area in part by process of vesiculation – loss free vesicles. In steady-state conditions, the number of vesicles is constant because of equilibrium between vesicles generated by erythrocytes and vesicles destructed by Kupffer cell mechanisms (Werre et al., 2004; Willekens et al., 2005).

The apparent rate of vesicle destruction at constant temperature can be described by first-order kinetics

$$\frac{dN}{dt} = -kN \quad (1)$$

where N is the concentration of vesicles being destructed, k represents the first-order rate constant, and t , the time of the thermal destruction. The solution of the equation (Eq.) (1) can be expressed as

$$N / N_0 = e^{-kt} \quad (2)$$

where N_0 is the initial concentration of vesicles and N/N_0 represents the ratio of the concentration of destructed vesicles to the initial vesicle concentration. This fraction defines the ratio of intact vesicles. Taking the logarithm of both sides of Eq. (2), one obtains

$$\log(N / N_0) = -2.303 \times kt \quad (3)$$

A plot of the left-hand side of Eq. (3) versus time (t) yields an estimate of k from the slope. The Arrhenius equation (Segel, 1976) can be used to express the temperature dependence of the first-order activation kinetics:

$$k = Ae^{-\frac{E_a}{RT}} \quad (4)$$

where R is the universal gas constant, E_a represents the apparent activation energy, and A -- the pre-exponential Arrhenius factor. Taking the logarithm of Eq. (4) yields:

$$\log k = -\frac{E_a}{2.303R} \times \frac{1}{T} + \log A \quad (5)$$

If the logarithm of k in Eq. (5) is plotted against the reciprocal of temperature, $1/T$, then the slope of this graph yields the activation energy (E_a), the thermal activation level of transitions from intact to destroyed

vesicle. The rate constant of the vesicle destruction process depends on the thermodynamic activation parameters of this transition state and can be described by the Eyring equation (Eyring et al., 1980):

$$k = \frac{k_b T}{h} e^{-\frac{\Delta G}{RT}} = \frac{k_b T}{h} e^{\frac{\Delta S}{R}} e^{-\frac{\Delta H}{RT}} \quad (6)$$

where k is the rate constant, ΔG is the standard Gibbs free energy of activation, h is Planck's constant, ΔS is the standard entropy of activation, ΔH is the standard enthalpy of activation, k_b is the Boltzmann constant, R is the gas constant, and T is the absolute temperature in Kelvin. Taking the logarithm of both sides of Eq. (6), one obtains:

$$\log\left(\frac{k}{T}\right) = \log\left(\frac{k_b}{h}\right) + \frac{\Delta S}{2.303R} - \frac{\Delta H}{2.303R} \times \frac{1}{T} \quad (7)$$

If the plot of the left-hand side of Eq. (7) versus $1/T$ is linear, one can compute the value of ΔH from the slope, ΔS from the ordinate intercept and the Gibbs free energy of activation by the relation:

$$\Delta G = \Delta H - T\Delta S \quad (8)$$

From Eq. 4 we can define the energy of activation as:

$$E_a = -R \frac{\partial \ln k}{\partial \left(\frac{1}{T}\right)} \quad (9)$$

The substitution of k in Eq. (9) with the k equivalent relation in Eq. (6) and differentiation of this new expression with respect to $1/T$ shows that the Arrhenius (Eq. 4) and the Eyring (Eq. 6) expressions can be related as:

$$E_a = \Delta H + RT \quad \text{and} \quad (10)$$

$$A = \left(\frac{ek_b T}{h}\right) e^{\frac{\Delta S}{R}} \quad (11)$$

Taking the logarithm of both sides of Eq.11, one obtains:

$$\log A = \log\left(\frac{ek_b T}{h}\right) + \frac{\Delta S}{2.303R} \quad (12)$$

suggesting a linear relation between the logarithm of the Arrhenius frequency factor and entropy of

activation obtained from the Eyring equation for the transitional state. The first-order kinetic model (Eq. 3) was used to determine the best fits of the data with the apparent rate constant k . The Arrhenius and Eyring equations were then applied to the data in order to determine E_a , A , ΔG , ΔH , and ΔS of the temperature-dependent viability transitions.

For two temperature points T_1 and T_2 it follows from Eq. 5 that

$$E_a = \frac{2.303T_1 T_2 \log \frac{k_2}{k_1}}{T_2 - T_1} \quad (13)$$

$$\log A = \log k_1 + \frac{E_a}{2.303R} \times \frac{1}{T_1} = \log k_2 + \frac{E_a}{2.303R} \times \frac{1}{T_2} \quad (14)$$

Substituting $\log A$ in Eq. 14 from Eq. 12 it follows that entropy

$$\Delta S = 2.303R \left[\log A - \log \frac{k_b}{h} - \log(eT) \right] \quad (15)$$

Enthalpy ΔH is found from Eq. 6 as

$$\Delta H = E_a - RT \quad (16)$$

Using ΔS from Eq. 15 and ΔH from Eq. 16, the Gibbs free energy of activation is calculated from Eq. 8.

2.4 Statistical analysis

T-test, linear regression, frequency and cumulative frequency, curve fitting and graph plotting were carried out using Microcal™ Origin version 6.0 (Northampton, MA) and 2010 Microsoft Excel. Geometric mean (μ_g) and geometric standard deviation (σ_g) for set of measured vesicle diameters (d_1, d_2, \dots, d_n) were calculated using the following equations (Wikipedia, 2012a):

$$\mu_g = \sqrt[n]{d_1 d_2 \dots d_n} \quad (17)$$

$$\sigma_g = \exp\left(\sqrt{\frac{\sum_{i=1}^n \left(\ln \frac{d_i}{\mu_g}\right)^2}{n}}\right) \quad (18)$$

Surface mean diameters (d_s) and volume mean diameters (d_v) of vesicles calculated from the count mean diameters (d) measured by light microscopy by using the following equations (Kethley et al., 1963):

$$\log d_s = \log d + 2.303 \log^2 \sigma_g \quad (19)$$

$$\log d_v = \log d + 6.908 \log^2 \sigma_g \quad (20)$$

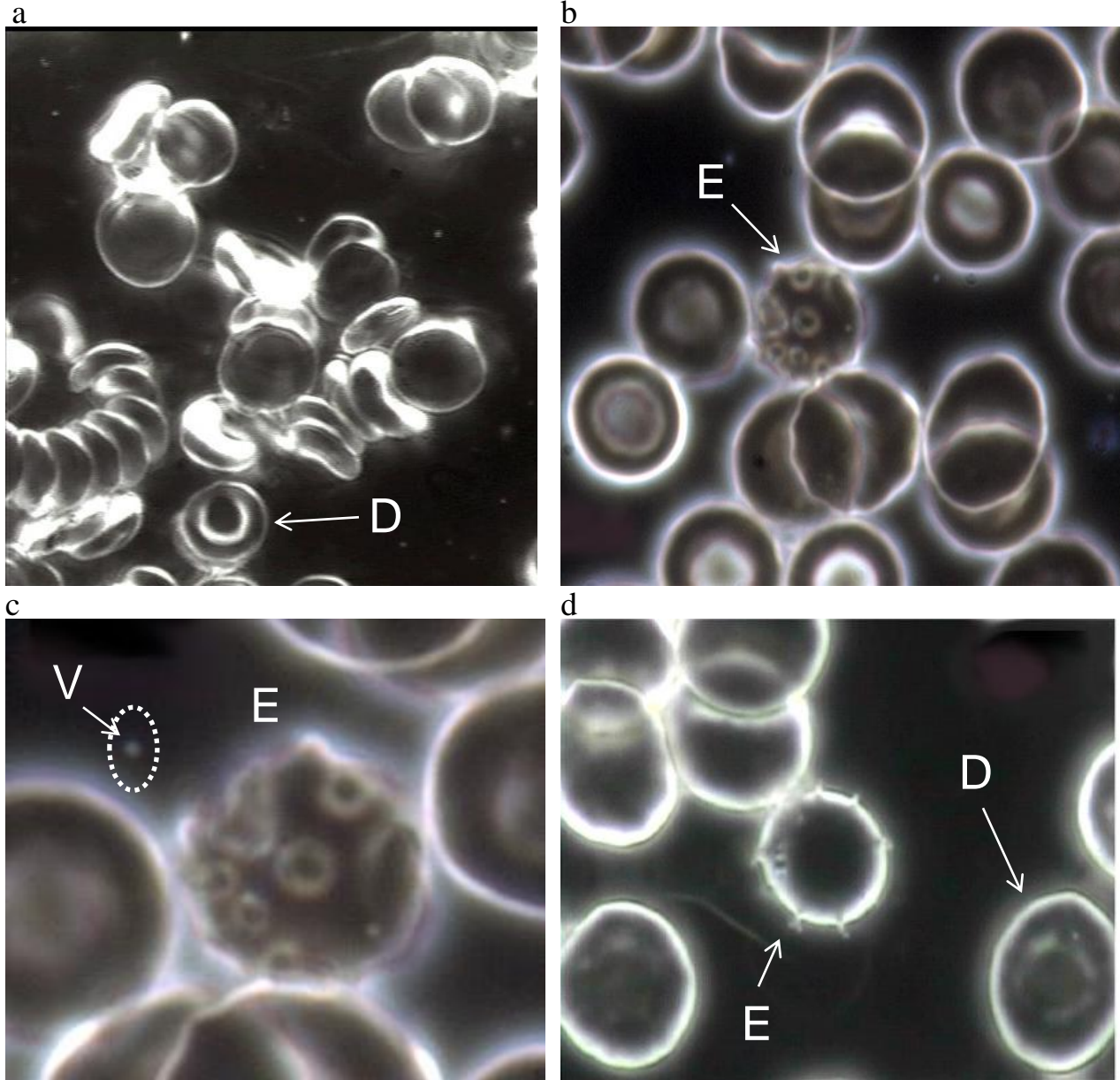


Fig. 1. Human erythrocytes transformation in blood samples at elevated temperatures induced by physical exercise. a. Erythrocytes before exercise at core temperature 37 °C. Most of the erythrocytes are double concave discs of ~7 microns in diameter. D- discocyte (normal biconcave discoid). b. Erythrocytes taken at core temperature of 38 °C after physical

exercise. Many erythrocytes are transformed into echinocytes (E) (crenated discs and spheres). c. Enlarged part of the frame b with echinocyte (E) in the middle. A free vesicle (V) is shown in a dashed circle. d. Another picture frame of erythrocytes taken at 38 °C after physical exercise. E – echinocyte (spiculated sphere).

3 Results

3.1 Erythrocyte-echinocyte transformation in blood

At the basal human core temperature of ~ 37 °C, erythrocytes in freshly drawn blood look as oval and

flexible biconcave discocytes with a diameter of ~7 μm (Fig. 1 a, Table 1).

When temperature rises due to physical exercise, some of the erythrocytes go through size and shape changes, being transformed into echinocytes. Starting with normal discocytes, they become crenated, and then assume spherical shape of smaller diameter with

Table 1. Erythrocyte statistics

Property	Human		Rat	
Life span	120 days	(Wikipedia, 2012b)	61 days	(Derelanko, 1987)
Diameter	7 μm	(Evans and Fung, 1972)	6.9 μm	(Canham et al., 1984)
Volume	90 μm^3	(Evans and Fung, 1972)	64.9 μm^3	(Canham et al., 1984)
Surface area	136 μm^2	(Evans and Fung, 1972)	103 μm^2	(Canham et al., 1984)
Concentration	$5 \times 10^6 \mu\text{L}^{-1}$	(Wikipedia, 2012b)	$8 \times 10^6 \mu\text{L}^{-1}$	(Willekens, 2010)
Total number	2.5×10^{13} (75 kg)	(Wikipedia, 2012b)	1.3×10^{11} (250 g)	(Lee and Blafox, 1985)
Blood volume	5 L (75 kg men)	(Wikipedia, 2012b)	16 mL (250 g rat)	(Lee and Blafox, 1985)

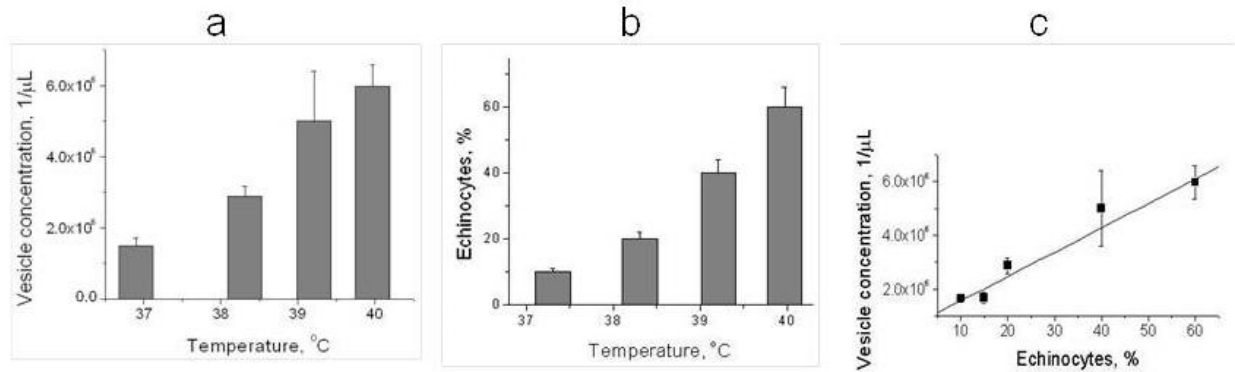


Fig. 2. Number of free vesicles is a function of echinocytes population in human blood. **a.** Mean number of vesicles in 1 μL of fresh blood taken before (at $\sim 37^\circ\text{C}$, core) and after physical exercise at maximal temperatures of $\sim 38, 39,$ and 40°C , core, respectively. **c.** Linear correlation between number echinocytes and vesicle concentration in blood. Points represent experimental data, while line is a linear fit ($R=0.95, P<0.012$).

fresh blood taken before (at $\sim 37^\circ\text{C}$, core) and after physical exercise at maximal temperatures of $\sim 38, 39,$ and 40°C , core, respectively. **c.** Linear correlation between number echinocytes and vesicle concentration in blood. Points represent experimental data, while line is a linear fit ($R=0.95, P<0.012$).

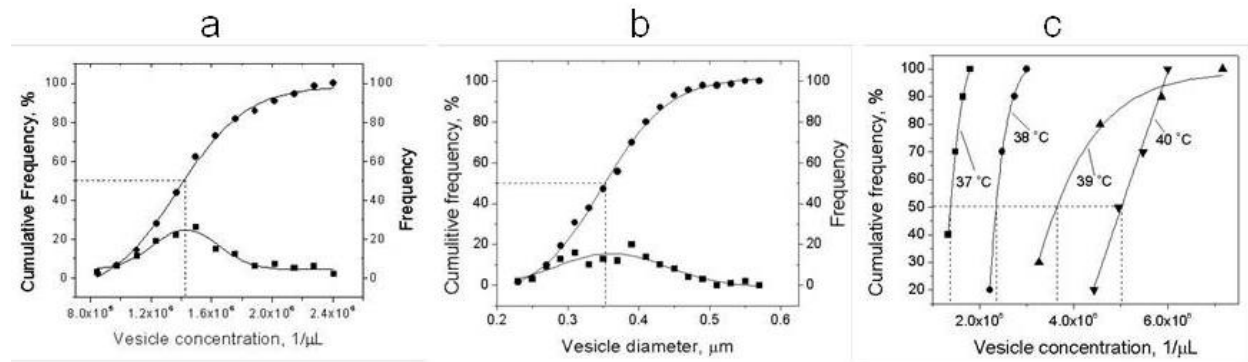


Fig. 3. Vesicle count and diameter distribution for human blood. **a.** Vesicle count distributions. Cumulative frequency distribution (●) and frequency count distribution (■) calculated from light microscopy images of non-fixed human blood at 37°C . The vesicle concentration at the maximum frequency count corresponds the 50% of the cumulative frequency. The points are experimental data while the cumulative frequency and the frequency count curves are the sigmoidal (Boltzmann) and the Gauss fits, respectively. Sigmoidal fit: $\text{Chi}^2=4.5, R^2=0.997$; Gauss fit: $\text{Chi}^2=4.0, R^2=0.948$. **b.** Vesicle diameter distributions. Cumulative frequency distribution (●) and frequency count distribution (■) calculated from light microscopy images of non-fixed

human blood at 37°C . The vesicle concentration at the maximum frequency count corresponds the 50% of the cumulative frequency. The points are experimental data while the cumulative frequency and the frequency count curves are the sigmoidal (Boltzmann) and the Gauss fits, respectively. Sigmoidal fit: $\text{Chi}^2=4.0, R^2=0.998$; Gauss fit: $\text{Chi}^2=7.7, R^2=0.828$. μm . **c.** Cumulative frequency distribution of vesicle concentration as function of temperature. The data were calculated from light microscopy images of non-fixed human blood at $37, 38, 39,$ and 40°C , respectively. The points are experimental data while the cumulative frequency curves are the sigmoidal (Boltzmann) fits. $R^2=0.996, 0.987, 0.993,$ and 0.994 for $37, 38, 39,$ and 40°C , respectively.

convex rounded protrusions (buds) (Fig. 1 b and c). The buds grow and finally fall off from the cell surfaces to become free vesicles. Some of the erythrocytes become spherical and grow spicules (Fig. 1 d). Vesicles bud off from the spicules. As temperature increases, the number of echinocytes and free vesicle increases. The images of rat erythrocytes before and after animals exposed to heat are very similar to those of human red blood cells prior to and after physical exercise (data not shown).

3.2 Statistics of vesicles shed by red blood cells

3.2.1 Vesiculation of human erythrocytes after exercise

The mean free vesicle concentration in blood after exercise as function of the human core temperature is shown in Fig. 2 a. The concentration is increased approximately 3 times as temperature rises from 37 to 40 °C. The percent of echinocytes in blood is also increased with elevated temperature (Fig. 2 b), so that there is a log-log linear correlation between vesicle concentration and present of erythrocyte-echinocyte transitions.

Fig. 3 a and b show frequency and cumulative frequency distributions of vesicle concentration and diameters at 37 °C, respectively. A mean vesicle concentration is $(1.51 \pm 0.35) \times 10^6$ vesicles/ μL with a mean diameter (d) is $0.365 \pm 0.065 \mu\text{m}$. A geometric standard deviation calculated by Eq 19 is equal to 1.20. The surface mean diameter (d_s) and volume mean diameters (d_v) of vesicles calculated by Eqs 19 and 20 are 0.377 and 0.403 μm , respectively.

Fig. 3 c compares cumulative frequency distribution of vesicle concentration at 37 °C (before exercise) and those at temperatures of 38, 39 and 40 °C (after exercise). When temperature increases the distribution moves towards higher vesicle concentrations. Vesicle concentration and diameter are shown in comparison with literature data in Table 2.

3.2.2 Vesiculation of rat erythrocytes after exposure to heat (passive hyperthermia)

The life span of human erythrocyte is only ~2 times longer than that of rats (Table 1) in spite of the rat's natural lifespan is about 20 times shorter (Alemán et al., 1998). Human and rat erythrocyte diameters are very comparable, volume and surface area about 25% large in humans, but concentration is 60% greater in rats. A general appearance of rat blood cells under high resolution microscope is very similar to one observed in

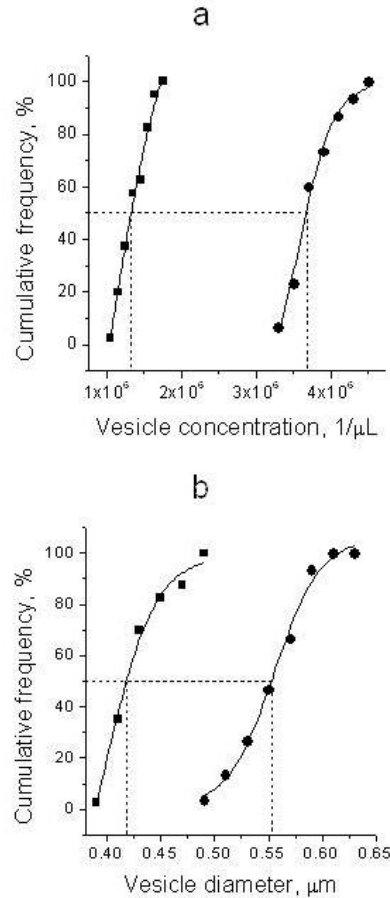


Fig. 4. Cumulative frequency distribution of vesicle concentration (a) vesicle diameter (b) at 36.7 (■) and 43.2 (●) °C. The data were calculated from light microscopy images of non-fixed rat blood before and after 25 min at 45 °C. The points are experimental data while the cumulative frequency curves are the sigmoidal (Boltzmann) fits. **a:** $R^2 = 0.993$ and 0.990, respectively; **b:** 0.991 and 0.994, respectively.

human samples (data not shown). As in the case with human erythrocytes, the concentration of free vesicles increase and is followed by the increase in erythrocyte-echinocyte transitions after exposure to heat stress. The concentration of free vesicles increased from $(1.4 \pm 0.2) \times 10^6$ to $(3.8 \pm 0.3) \times 10^6$ vesicles/ μL .

The rat temperature measured in the ear is assumed to be 2.5 degree lower than the rat core temperature (Briese, 1998; Vianna and Carrive, 2005) and increased during a heat exposure from 36.7 to 43.2 °C. Fig. 4 shows frequency and cumulative frequency distributions of vesicle concentration and diameter. The figure indicates a significant shift to higher vesicle concentrations and diameter after a heat stress. The mean vesicle diameter at 36.7 °C is $0.436 \pm 0.03 \mu\text{m}$, and at 43.2 °C is $0.559 \pm 0.03 \mu\text{m}$. A geometric standard deviation calculated by Eq 19 is equal to 1.06. At 36.7 °C, the surface mean diameter (d_s) and volume mean

Table 2. Vesicle concentration (C) and diameter (d)

Subject	Condition	Method	t, °C	C, μL^{-1}	d, μm	Reference
Human	Live	Light microscopy	37	1.5×10^6	0.365	Present work
Rat	Live	Light microscopy	36.7	1.4×10^6	0.436	Present work
Human	Storage, 5 days	Flow cytometry	4	3,370	<1	(Rubin et al., 2008)
Human	Storage, 50 days	Flow cytometry	4	64,850	<1	(Rubin et al., 2008)
Human	Fixed	Flow cytometry	37	170	0.5	(Willekens et al., 2008)
Human	Centrifuged	Flow cytometry	37	28	ND	(Berckmans et al., 2001)
Human	Centrifuged	Flow cytometry	37	192	ND	(Shet et al., 2003)

ND-not determined

Table 3. Thermodynamic analysis of erythrocyte hemolysis and vesiculation

Process	T °C	Activation energy, E_a , KJ.mol^{-1}	Enthalpy ΔH , KJ.mol^{-1}	Entropy ΔS , $\text{J.mol}^{-1}\text{K}^{-1}$	Entropy contribution $T\Delta S$, KJ.mol^{-1}	Free energy, ΔG , KJ.mol^{-1}
Increase of number of vesicles in blood as result of the human core temperature increase during exercise ¹	37-39	776.1	773.5	2,342	728.3	45.2
Increase of vesicles in rat blood as result of environmental heating at 45 °C for 25 minutes ¹ .	36.7-43.2	427.4	424.8	1,240	387.6	35.1
K ⁺ release from erythrocytes <i>in vitro</i> ² vesiculation	19-37	63.5	66.4	-19.5	-24.6	91.0
AchE release during vesiculation <i>in vitro</i> ²	19-37	63.5	60.9	-20.9	-26.4	87.3
Formation of methemoglobin in erythrocytes <i>in vitro</i> ²	19-37	129.6	127.0	29.8	37.2	89.5
Basal ion permeability in erythrocytes <i>in vitro</i> ³	37-57	102.0	99.0	-5.7	-7.6	106.6
Erythrocyte osmotic fragility ⁴	48-49	2400	2401	7,167	2,305	96.0
Erythrocyte hemolysis ⁵	38-45	131.7	129.1	71.5	22.5	106.6
Erythrocyte hemolysis ⁵	45-50	342	339.1	346	234.5	104.6
Erythrocyte hemolysis ⁶	38-45	290	286	536	174	112
Discocyte-echinocyte transition ⁷	15-35	206.1	71.9	-10.9	-12.5	84.4
Heat survival of CHO cells in cultures ⁸	41-43	1266	1264	3,736	1,178	86

1. Present work. 2. (Chernitskii et al., 1994). 3. (Ivanov et al., 2007) 4. (Ham et al., 1948) 5. (Gershfeld and Murayama, 1988) 6. (Przybylska et al., 2000) 7. (Glaser, 1979) 10. (Bauer and Henle, 1979)

diameters (d_v) of vesicles calculated by Eqs 19 and 20 are 0.438 and 0.441 μm , respectively.

3.3 Thermodynamics of erythrocyte vesiculation

3.3.1 Human case study

When human core temperature rises during exercise from 37 to 38, 37 to 39, and 37 to 40 °C, the change of relative vesicle concentration per minute (apparent rate constant, k) is found to be 8.17×10^{-3} , 2.22×10^{-2} , and $4.46 \times 10^{-2} \text{ min}^{-1}$, respectively. The graph of the logarithm of the rate constants as function of $1000/T$ (Eq 5) represents the Arrhenius plot shown in Fig. 5 a. The slope of the plot yields the activation energy (E_a), the thermal activation level of vesiculation and $\log A$

from the ordinate intersect. The same rate constants were used to generate the Eyring plots shown in Fig. 5 b. The linear plot of the left-hand side of Eq 7 vs $1/T$ brings the value of ΔH from the slope, ΔS from the ordinate intercept and the Gibbs free energy of activation (ΔG) by Eq 8. Activation energy (E_a) and ΔS can be calculated by a second way from Eqs 10 and 12. The calculated values of E_a , ΔH , ΔS , and ΔG for process of human erythrocyte vesiculation are shown in Table 3.

3.3.2 Rats

Rat erythrocytes lose 30% of volume during its lifespan (Willekens, 2010). Taking rat erythrocyte volume from Table 1, the lost volume, $L_v = 0.3 \times 64.9 \mu\text{m}^3 = 19.47 \mu\text{m}^3$. The volume of a single vesicle (v) is estimated as

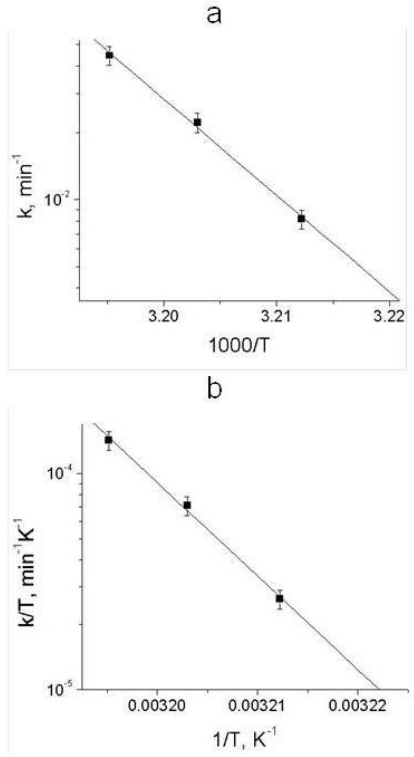


Fig. 5. Estimation of vesicle thermodynamic properties by Arrhenius and Eyring equations. **a.** Arrhenius plot. Points are experimental data plotted by Eq 5, line is a linear regression: $R=-0.999$, $P<0.04$. **b.** Eyring plot. Points are experimental data plotted by Eq 7 and line is a linear regression. $R=-.999$, $P<0.04$.

$v=\pi d_v^3/6=\pi(0.441)^3=4.49\times 10^{-2}\ \mu\text{m}^3$. If all lost erythrocyte volume is converted to vesicles, the number of produced vesicles during the erythrocyte lifespan $n=L/v=19.47\ \mu\text{m}^3/4.49\times 10^{-2}\ \mu\text{m}^3=434$.

If the surface area of a single vesicle, $s=\pi d_s^2=\pi(0.438)^2=0.602\ \mu\text{m}^2$, the total area (S) of 434 vesicles would be equal to $434\times 0.602\ \mu\text{m}^2=261\ \mu\text{m}^2$ that is much higher than the whole area of erythrocyte ($103\ \mu\text{m}^2$). During a lifespan, erythrocytes reduce their surface area by 20% (Willekens, 2010), which amounts to the area loss $L_s=0.2\times 103\ \mu\text{m}^2=20.6\ \mu\text{m}^2$. Comparing the estimated total area $S=261\ \mu\text{m}^2$ to the experimental loss $L_s=20.6\ \mu\text{m}^2$, one can conclude that only $20.6/261\approx 8\%$ of lost area are converted to vesicles. 8% of the lost erythrocyte volume $V=8\%\times L_v=0.8\times 19.47\ \mu\text{m}^3=1.54\ \mu\text{m}^3$. Then, number of vesicles produced by a single erythrocyte during its lifespan, $n=V/v=1.54\ \mu\text{m}^3/4.49\times 10^{-2}\ \mu\text{m}^3=34.22$. Taking in account total number of erythrocytes is 1.3×10^{11} and lifespan is 61 days (Table 1), it follows that vesicle destruction rate at basal temperature of $36.7\ ^\circ\text{C}$, $k_1=1.3\times 10^{11}\times 34.22:61:24:60\approx 5.0\times 10^7\ \text{min}^{-1}$.

When the rat is exposed to heat, the rat core temperature increases from $t_1=36.7$ to $t_2=43.2\ ^\circ\text{C}$, vesicle concentration rises from 1.4×10^6 to 3.8×10^6 vesicles/ μL (Section 3.2.2). Taking in account the duration of hyperthermia (25 min) and rat blood volume (16 mL) (Table 1), the vesicle destruction rate (k_2) at the transition from t_1 to t_2 can be estimated as following

$$k_2=(3.8\times 10^6-1.4\times 10^6)\ \text{vesicles}/\mu\text{L}\times 1.6\times 10^4\ \mu\text{L}/25\ \text{min}=1.54\times 10^9\ \text{min}^{-1}.$$

Using values of k_1 and k_2 at absolute temperatures T_1 and T_2 and Eq. 13, one can estimate the apparent activation energy $E_a=427.4\ \text{kJmol}^{-1}$.

A value of $\log A$ calculated by Eq 14 and inserted in Eq 15 allows calculation of entropy change (ΔS) at temperature $T=(T_1+T_2)/2=(309.7+316.2)/2\approx 313\ \text{K}$ ($40\ ^\circ\text{C}$). ΔS is found to be equal to $1240\ \text{Jmol}^{-1}\text{K}^{-1}$.

Inserting values of E_a and RT in Eq 16, one can calculate enthalpy change $\Delta H=424.8\ \text{kJmol}^{-1}$.

Finally, substituting ΔH and ΔS in Eq 8 with found above values, it follows that free Gibbs energy (ΔG) is equal to $35.1\ \text{kJmol}^{-1}$. The calculated values of E_a , ΔH , ΔS , and ΔG for process of rat erythrocyte vesiculation are shown in Table 3.

3.3.3 Thermodynamic correlates of erythrocyte vesiculation

When enthalpy change (ΔH) for vesiculation of human and rat erythrocytes obtained in this work together with ΔH related to other phenomena related to the thermal cell decomposition given in Table 3 were plotted as function of entropy change (ΔS), the data were fitted with a single line that corresponds to the equation $\Delta H=\Delta G_o+T_o\Delta S$, where $\Delta G_o=96.5\ \text{kJxmol}^{-1}$ and $T_o=317\ ^\circ\text{K}$ (Fig.6).

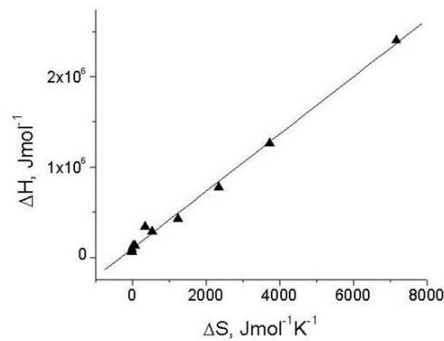


Fig. 6. Thermodynamic correlation of enthalpy and entropy for erythrocyte degradation. Points are experimental and literature data (Table 3), while a line is a linear regression: $R=0.997$, $P<0.0001$.

4 Discussion

4.1 Light microscopy of live cells and vesicles

The introduction of no-label high resolution light microscopy gave new opportunity for live cell analysis, including capability of visualizing and recording of cell events at the submicron scale. In the newly developed light system, the object is illuminated by the focused hollow cone of light (instead of beam of light). The effect of the annular illumination promotes the narrowing of the central spot of diffraction pattern and increase of the intensity of the diffraction fringes. The similar effect of annular aperture is known and used in telescopes (Born and Wolf, 1999) to increase the resolution. A better than 90 nm resolution of the Richardson plate (Richardson, 1988) line and picture patterns has been achieved (Foster, 2004; Vainrub et al., 2006; Vodyanoy, 2005; Vodyanoy et al., 2007). The high resolution microscopic illumination system was commercialized and it is known as CytoViva. It is broadly used in live cell and nanoparticle analysis (Asharani et al., 2010; Carlson et al., 2008; Jayachandran et al., 2008; Jun et al., 2012; Lim et al., 2012; Rahimi et al., 2008; Shiekh et al., 2010; Weinkauff and Brehm-Stecher, 2009).

Light images of rat blood cells shown in this work are taken within a few minutes after small samples (<10uL) are drawn. The samples are not subjected any chemical treatments. The cells are videotaped in the natural environment and selective frames are shown in Fig. 1 and 7. The high resolution optical images of human erythrocytes, echinocytes, and free vesicles are consistent with those obtained by electron microscopy (Bessis, 1972; Brecher and Bessis, 1972; Christel and Little, 1984; Dumaswala and Greenwalt, 1984; Longster et al., 1972; Orozco and Lewis, 2010; Repin et al., 2008). The chief advantages of high resolution light microscopy utilized in this work compared to scanning electron microscopy lies in the ability to image live cells in real time at a lower cost. This technique is especially important for free moving vesicles because it allows their discrimination from background.

In this work, vesicle concentrations found in rat and human freshly drawn blood samples at basal conditions found to be at the level of 10^6 vesicles/ μ L. This concentration is a few orders of magnitude higher than those found in literature (Table 2). It is well recognized that there is a substantial amount of variation between researchers regarding the preparation procedures used in isolating erythrocyte vesicles, with essential differences in anticoagulants, filtration, centrifugation and flow cytometry, which frequently result in data variability (Dey-Hazra et al., 2010; Hind et al., 2010;

Huica et al., 2011). Most of the erythrocyte vesicles are ranged in between 0.1 and 1 μ m (Hind et al., 2010), but the most traditional detection technique, flow cytometry, has a detection threshold in the range of 0.4-0.5 μ m. The cumulative frequency analysis of vesicle diameters showed that 80% of all vesicles found in blood are smaller than 0.4 μ m (Fig. 3 b). It is therefore concluded that majority of vesicles are lost during preparation and detection.

4.2 Erythrocyte vesiculation at elevated temperatures

Flow cytometry studies demonstrated that vesicles derive mostly from erythrocytes (approximately 65%) (Willekens, 2010). Human and rat erythrocytes have quite similar physical properties (Table 1). Basal properties including core temperature, vesicle concentration and diameter are very comparable (table 2). When the rat is exposed to environmental hyperthermia, the core temperature and the concentration of free vesicles in the blood increase following the rise of the erythrocyte – echinocyte transitions. This fact is in very good agreement with *in vivo* experiments involving blood and isolated erythrocytes subjected to heat (Araki et al., 1982; Chernitskii et al., 1994; Christel and Little, 1984; Glaser, 1979; Glaser and Donath, 1992; Leonards and Ohki, 1983; Repin et al., 2008; Rumsby et al., 1977; Schultze, 1865; Wagner et al., 1986); and also with erythrocytes involved in burns (Baar and Arrowsmith, 1970; Brown, 1946; Loebel et al., 1973; Vtiurin et al., 1987). It is well established that the increased metabolic heat of physical exercise causes a rise of core temperature in human and animals (Briese, 1998; Greenleaf, 1979; Nybo and Nielsen, 2001a; Parrott et al., 1999; Periard et al., 2012; Sawka and Wenger, 1988; Walsh and Whitham, 2006; White and Cabanac, 1996). In this work, the elevated temperature due to physical exercise in human is accompanied by both the increase in number of transformed erythrocytes (echinocytes) and rise of free vesicle concentration. The thermodynamic analyses of free vesicles in rat and human live blood samples was implemented with the premise that temperature and corresponding energy, enthalpy, and entropy are responsible for red blood cells vesiculation. Obtained thermodynamic data for rat environmental hyperthermia and human exercise induced temperature increase are consistent with each other and agree well with thermodynamic literature results (Chernitskii et al., 1994; Gershfeld and Murayama, 1988; Glaser, 1979; Ham et al., 1948; Ivanov, 2007; Ivanov et al., 2007; Przybylska et al., 2000). Although, all external conditions but temperature were kept the same, the heat stress alone could be suggested as an essential but not the only

factor in red blood cell vesiculation. Other stressors may be involved. This situation is similar to another heat stress phenomenon: exercise-increased extracellular heat shock protein 72 (eHsp72) levels. It was shown in rats (Ogura et al., 2008) and human subjects (Whitham et al., 2007), that body temperature increase during physical exercise is essential for activation of exercise-increased eHsp72. However, exercise-related stressors other than heat seemed important in exciting HSP72 release.

A human erythrocyte loses $15 \mu\text{m}^3$ of volume during its lifespan (120 days) (Bosman et al., 2008). The volume of a single vesicle (v) is estimated as $v = \pi d_v^3 / 6 = \pi(0.403)^3 = 3.43 \times 10^{-2} \mu\text{m}^3$. If all lost erythrocyte volume (L) is converted to vesicles, the number of produced vesicles (n) during the erythrocyte lifespan $n = L/v = 19.47 \mu\text{m}^3 / 4.49 \times 10^{-2} \mu\text{m}^3 = 437$.

If surface area of a single vesicle, $s = \pi d_s^2 = \pi(0.377)^2 = 0.446 \mu\text{m}^2$, the total area (S) of 437 vesicles would be equal to $437 \times 0.446 \mu\text{m}^2 = 194 \mu\text{m}^2$ that is much higher than the whole area of erythrocyte ($136 \mu\text{m}^2$). During a lifespan, erythrocyte reduces its surface area by 20% (Werre et al., 2004), what amounts to the area loss $L_s = 0.2 \times 136 \mu\text{m}^2 = 27.2 \mu\text{m}^2$. Comparing the estimated total area $S = 194 \mu\text{m}^2$ to the experimental loss $L_s = 27.2 \mu\text{m}^2$, one can conclude that only $27.2/261 \approx 14\%$ of lost area are converted to vesicles. Similar estimate made for rat erythrocytes (Section 3.3.2) shows that only 8% of lost erythrocyte material is lost by shedding vesicles. At average, both rat and human red blood cells shed one vesicle every two days during their lifespan. It means that 86% of the lost human erythrocyte material and 92% of rat erythrocyte are lost not by vesiculation but by another unknown mechanism.

A similar analysis of the lifespan loss of human erythrocyte volume and surface area was carried out based on experimental results obtained by centrifugation and flow cytometry (Werre et al., 2004; Willekens et al., 2008). They found a strong discrepancy between estimated and observed loss of erythrocyte surface area. Authors concluded: "Taken together, these data suggest that most vesicles are taken up almost directly by the macrophages of the organ in which they originate before they can reach the venous circulation and be counted. Apparently, the body has developed an efficient mechanism to remove these vesicles..." (Willekens et al., 2008; Willekens, 2010). Being not aware of the direct removal mechanism of hemoglobin by macrophages, the authors explained the extra loss of surface area in comparison to the hemoglobin loss by incorporation of lipids (Bosman et al., 2008). This explanation seems not very likely,

because during erythrocyte aging, cell loses 20% of lipids that is equal to a loss of hemoglobin (Rumsby et al., 1977). We hypothesize, that an alternative mechanism of direct transfer of damaged hemoglobin does exist but remains unknown.

During observation and video recording of fresh samples of live blood, direct and prolong contacts between echinocytes and white cells are frequently accounted. In contrast, white cells were not observed in contact with intact erythrocytes. When white cells approach erythrocytes, the cells repulse and scatter. We speculate that during such contacts with echinocytes, peripherally located membrane buds are directly scavenged by white cells. Fig. 7 shows a single frame of a video recording of echinocytes that may be engaged in process of removal of surface vesicles by white cells. The figure also shows also many free vesicles and erythrocytes. The facts of the selective interaction of white cell with echinocytes and the avoidance of erythrocytes are substantiated by the difference in surface electric charges. It has been demonstrated that negative surface electrical charge of aging red blood cells is reduced (Huang et al., 2011). White blood cells have a negative surface charge (Gallin, 1980), therefore the reduction of the aging erythrocyte charge reduces repulsive forces and promotes adhesiveness.

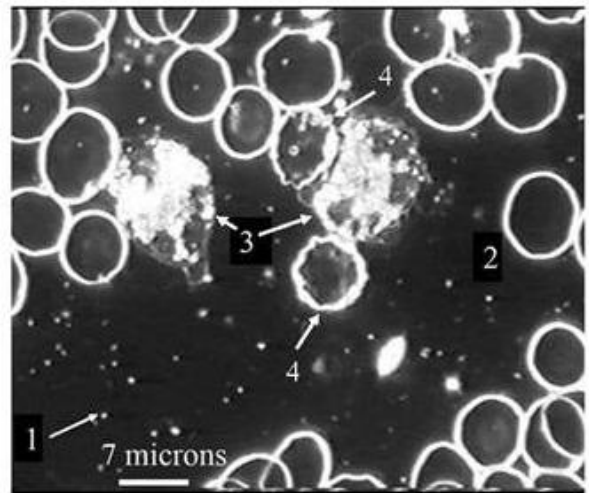


Fig. 7. Direct contact of white and red blood cells in human blood. 1-vesicle; 2-erythrocyte; 3-neutrophil, 4-echinocytes; 100X objective, oil.

The thermodynamic data include results on rat and human red blood cell vesiculation (obtained in this work), data on individual steps of erythrocyte vesiculation process, and heat survival of Chinese hamster ovary cells (Table 3 and Fig. 6).

It is accepted that intracellular erythrocyte oxidation of hemoglobin into methemoglobin leads to ATP depletion with follow on dephosphorylation of membrane proteins and lipids (Vittori et al., 2012). The change of K^+ and Cl^- membrane permeability causes the loss of KCl and osmotically driven water, which in turn leads to cell contraction, externalization of phosphatidylserine (the processes specific to eryptosis) (Lang and Qadri, 2012) and erythrocyte-echinocyte transitions (Backman, 1986). It has been demonstrated that during vesiculation of human erythrocytes *in vitro*, acetylcholinesterase redistributes on the cell surface and becomes enriched in the released vesicles (Butikofer et al., 1989; Lutz et al., 1977). Additionally, it was shown that acetylcholinesterase (AChE) release correlates with vesiculation of red blood cells (Wagner et al., 1986). It is important to note that process of erythrocyte hemolysis, leads to cell death, but it is very different from the programmed cell death – eryptosis. The main difference lies in the fact that during hemolysis the osmotically driven water moves inside cell, causing it to swell and break it apart, while in eryptosis, water moves outside, causes cell shrinkage and vesiculation. The hemolysis is an adverse cell phenomenon, but eryptosis allows defective erythrocytes to escape hemolysis and prolongs cell life (Föller et al., 2008). When erythrocytes are subjected to hypotonic solution, as in osmotic fragility test (Ham et al., 1948), the cells experience morphological changes that are similar to those during a normal eryptosis. Under influence of osmotic pressure, water moves from inside out, and forces the cells to experience remarkable changes: the first is the appearance of small bud-like protrusions on an occasional erythrocyte; the next recognizable change, many of the erythrocytes show single or multiple buds; then many erythrocytes are converted to spheroid cells, and finally, buds are pinched off creating many free vesicles of one micron and smaller in sizes (Ham et al., 1948).

The change of enthalpy is positive, $\Delta H > 0$ for all experiments (Table 3) indicating that all examined processes related to vesiculation and hemolysis are endothermic, i.e. they occur with adsorption of heat. The enthalpy change observed in human erythrocytes due to temperature elevated by exercise is larger than ΔH in rat exposed to heat. The highest value of ΔH is observed in the erythrocyte osmotic fragility. It is larger than ΔH observed in this work. A few conditions of the osmotic fragility experiment are different from those of this work. The osmotic fragility tests are *in vitro* experiments when erythrocytes are isolated and then exposed to hypotonic solutions and elevated temperatures. In experiments of this work, red blood cells are challenged with elevated temperatures while they are *in vivo*. One can speculate that being *in vivo*,

erythrocytes may use ATP internal energy to undertake steps leading to change of membrane ion permeability and create osmotic compression. It would save the thermal energy that breaks cells. In contrast, in osmotic fragility experiment, the ATP component is missing and therefore, a higher enthalpy is required to vesiculate cells. A much smaller ΔH observed in hemolysis of erythrocytes when osmotic pressure drives water inside the cell and swells it. The smaller ΔH required for cell hemolysis agrees well with the fact that model vesicles can withstand smaller stretching than compressive osmotic pressures (Oglecka et al., 2012). The important step of vesiculation, discocyte-echinocyte transition, has a relatively small ΔH that is about the same values as enthalpies of K^+ and AChE release from erythrocytes during vesiculation.

The values of $T\Delta S$ in Table 3 ranges from -26.4 to 2,305 $KJmol^{-1}$ and for each process they are comparable with the enthalpy change ΔH . Entropies (ΔS) of the ion permeability change and K^+ -ion and AChE release from erythrocytes during vesiculation are found to be negative. $\Delta S < 0$ has conventionally been associated with decreases in molecular rotational and translational degrees of freedom. $\Delta S < 0$ in processes involving aqueous solvents often involves the dehydration of solvent moieties forming the interface between the contacting molecules and by release of ions (Dragan et al., 2003). A discocyte-echinocyte transition is also shows a negative entropy change. The appearance of protrusions on the surface of echinocytes, increases the cell membrane curvature and consequently, increases entropy (Beck, 1978). As result, the discocyte-echinocyte transition is accompanied with the negative entropy change.

The energy associated with the change of entropy, $T\Delta S$, correlates with the change of enthalpy, ΔH , keeping the Gibbs free energy, $\Delta G = \Delta H - T\Delta S$, and small compared to both ΔH and $T\Delta S$. This thermodynamic phenomenon is known as enthalpy-entropy compensation (Leffler, 1955; Tomlinson, 1983) The enthalpy-entropy compensation phenomenon is characteristically displayed by a linear graph of ΔH vs. ΔS as revealed in these studies when the experimental data across different results related to red blood cells destruction were grouped in Table 3 and Fig. 6. The ΔH versus ΔS results are consistent with the linear free energy relations ($r = 0.997$, $p < 0.0001$) of a characteristic enthalpy–entropy compensation plot, with the slope approximating the mean temperature of the range of temperatures used in the experiments.

The joint influence of a small temperature range of apparent rates of destruction and the alteration of

coordinates can result in entirely mistaken associations between ΔS and ΔH (Sharp, 2001). In present work, nevertheless, the parameters were determined not separately from pairs of rate data, but obtained by regression analysis of Arrhenius plots that incorporated several rate measurements at the relatively large temperature range of 15-57° C; most of the time the slopes were statistically significant at the 1-4 % level of probability. Since the correlation shown in Fig. 6 is highly significant ($P = 0.0001$), it is concluded that it is a correct presentation of the compensation law. According to accepted interpretation data like this, this result means that with exception of CHO data, mechanisms of erythrocyte hemolysis and vesiculation is identical for the cells irrespectively of subjects. The suggestion that apparent rates associated with erythrocyte vesiculation, hemolysis, K^+ and AchE release, ion permeability, formation of methemoglobin, osmotic fragility, discocyte-echinocyte transition, and CHO heat survival of three different species follow the same mechanism is hard to accept. Nevertheless, all processes include a common substance: they all involve water. Therefore, it is deduced that the ΔS - ΔH correlation shown here relies more upon the physical state of water molecules in cell membrane. This explanation is in agreement with the conclusion made in the study of erythrocyte hemolysis of man, rabbits, guinea-pigs, rats, sheep, cats and pigs (Good, 1967). It is also consistent with deduction of Ives and Marsden, who suggested that for chemical systems the compensation law is most often seen in reactions that vary from each other primarily in the degree to which solvational changes may take place (Ives and Marsden, 1965). More recently, solvent reorganization was suggested as a driving force for encapsulation in water, that can be revealed enthalpy-entropy compensation (Leung et al., 2008). Lipid as a common component of all cell membranes (Yeagle, 1989), is present in all erythrocytes, vesicles, and other cells analyzed in this work. It was demonstrated that hydration highly impacts the molecular and electronic structure of membrane phospholipids and therefore direct the interactions of the lipids with other molecules and strongly contribute to physical properties of membrane (Mashaghi et al., 2012). Thus we speculate that the common mechanism of the ΔS - ΔH compensation plot may therefore include the hydration state of membrane phospholipid.

4.3 Diagnostic value of erythrocyte vesicles

During physical exercise, body temperature is elevated (Buono et al., 2005; Ogura et al., 2008). One of the serious consequences of a mild increase of temperature (~ 38 °C) is energy depletion (Kozlowski et al., 1985).

That is in turn results in the accelerated erythrocyte-echinocyte transition (Backman, 1986; Brecher and Bessis, 1972) and increased vesicle shedding from speculated cells (Christel and Little, 1984). At temperatures higher than 38 °C, a cell's hemolysis comes into effect, and vesicle production grows as temperature increases (Gershfeld and Murayama, 1988). It is therefore, hypothesized that increase of vesicle number related to elevated temperatures during exercise may serve as diagnostic of erythrocyte stability. Because the decreased stability of red blood cells reduces their capability of oxygen transport (Nybo et al., 2001; Nybo et al., 2002; Nybo and Nielsen, 2001b), impairs endurance, and causes fatigue (El-Sayed et al., 2005; Periard et al., 2011), the number of vesicles increases due to exercise may be examined for its diagnostic value of human performance.

5 Conclusions

1. High resolution light microscopy of live blood cells is an appropriate technique for imaging heat induced structural erythrocyte transformations and vesicle release.
2. Vesicle release accounts for only a small part of erythrocyte surface reduction during its lifespan. It is suggested that a large part of the aged erythrocyte membrane is removed by direct contacts with white cells.
3. Entropy-enthalpy compensation is associated with erythrocyte-echinocyte transitions at elevated temperatures and is assumed to include the hydration state of membrane lipid.
4. Physical exercise results in elevation of body temperature, energy depletion, acceleration of erythrocyte-echinocyte transition, and in turn increases the number of released vesicles. These changes reduce erythrocyte stability, capability of oxygen transport, impair endurance, and cause fatigue. Therefore, the number of vesicles released increases due to exercise and therefore has a diagnostic value of human performance.

Acknowledgements

Authors are grateful to members of Department of Anatomy, Physiology and Pharmacology and Department of Kinesiology of Auburn University for support and encouragement.

References

- Alemáan, C.L., Más, R.M., Rodeiro, I., Noa, M., Hernández, C., Menéndez, R., Gámez, R., 1998. Reference database of the main physiological parameters in Sprague-Dawley rats from 6 to 32 months. *Laboratory Animals* 32, 457-466.
- Araki, T., Roelofsen, B., Op Den Kamp, J.A.F., van Deenen, L.L.M., 1982. Temperature-dependent vesiculation of human erythrocytes caused by hypertonic salt: A phenomenon involving lipid segregation. *Cryobiology* 19, 353-361.
- Asharani, P.V., Sethu, S., Vadukumpully, S., Zhong, S., Lim, C.T., Hande, M.P., Valiyaveetil, S., 2010. Investigations on the Structural Damage in Human Erythrocytes Exposed to Silver, Gold, and Platinum Nanoparticles. *Advanced Functional Materials* 20, 1233-1242.
- Baar, S., 1974. Mechanisms of delayed red cell destruction after thermal injury. An experimental in vitro sem study. *Br J Exp Pathol* 55, 187-193.
- Baar, S., Arrowsmith, D.J., 1970. Thermal damage to red cells. *J Clin Pathol* 23, 572-576.
- Backman, L., 1986. Shape control in the human red cell. *J Cell Sci* 80, 281-298.
- Bauer, K.D., Henle, K.J., 1979. Arrhenius Analysis of Heat Survival Curves from Normal and Thermotolerant CHO Cells. *Radiation Research* 78, 251-263.
- Beck, J.S., 1978. Echinocyte formation: A test case for mechanisms of cell shape changes. *Journal of Theoretical Biology* 71, 515-524.
- Berckmans, R.J., Nieuwland, R., Boing, A.N., Romijn, F.P., Hack, C.E., Sturk, A., 2001. Cell-derived microparticles circulate in healthy humans and support low grade thrombin generation. *Thromb Haemost* 85, 639-646.
- Bessis, M., 1972. Red cell shapes. An illustrated classification and its rationale. *Nouv Rev Fr Hematol* 12, 721-745.
- Born, M., Wolf, E., 1999. *Principles of Optics*, 7th ed. U. Press, Cambridge.
- Bosman, G., Werre, J.M., Willekens, F.L.A., Novotny, V.M.J., 2008. Erythrocyte ageing in vivo and in vitro: structural aspects and implications for transfusion. *Transfusion Medicine* 18, 335-347.
- Bosman, G.J., Cluitmans, J.C., Groenen, Y.A., Werre, J.M., Willekens, F.L., Novotny, V.M., 2011. Susceptibility to hyperosmotic stress-induced phosphatidylserine exposure increases during red blood cell storage. *Transfusion* 51, 1072-1078.
- Bratosin, D., Estaquier, J., Petit, F., Arnoult, D., Quatannens, B., Tissier, J.P., Slomianny, C., Sartiaux, C., Alonso, C., Huart, J.J., Montreuil, J., Ameisen, J.C., 2001. Programmed cell death in mature erythrocytes: a model for investigating death effector pathways operating in the absence of mitochondria. *Cell death and differentiation* 8, 1143-1156.
- Brecher, G., Bessis, M., 1972. Present Status of Spiculed Red Cells and Their Relationship to the Discocyte-Echinocyte Transformation: A Critical Review. *Blood* 40, 333-344.
- Briese, E., 1998. Normal body temperature of rats: the setpoint controversy. *Neuroscience & Biobehavioral Reviews* 22, 427-436.
- Brown, A., 1946. Morphological changes in the red cells in relation to severe burns. *The Journal of Pathology and Bacteriology* 58, 367-372.
- Buono, M.J., Barrack, M.T., Bouton-Sander, F., Bradley, P., Cottonaro, K.A.M., 2005. Effect of exercise-induced hyperthermia on serum iron concentration. *Biological Trace Element Research* 108, 61-68.
- Burnier, L., Fontana, P., Kwak, B.R., Angelillo-Scherer, A., 2009. Cell-derived microparticles in haemostasis and vascular medicine. *Thrombosis and Haemostasis* 101, 439-451.
- Butikofer, P., Kuypers, F.A., Xu, C.M., Chiu, D.T., Lubin, B., 1989. Enrichment of two glycosyl-phosphatidylinositol-anchored proteins, acetylcholinesterase and decay accelerating factor, in vesicles released from human red blood cells. *Blood* 74, 1481-1485.
- Canham, P.B., Potter, R.F., Woo, D., 1984. Geometric accommodation between the dimensions of erythrocytes and the calibre of heart and muscle capillaries in the rat. *The Journal of Physiology* 347, 697-712.
- Carlson, C., Hussain, S.M., Schrand, A.M., Braydich-Stolle, L.K., Hess, K.L., Jones, R.L., Schlager, J.J., 2008. Unique cellular interaction of silver nanoparticles: size-dependent generation of reactive oxygen species. *The journal of physical chemistry. B* 112, 13608-13619.
- Castellana, D., Toti, F., Freyssinet, J.-M., 2010. Membrane microvesicles: Macromessengers in cancer disease and progression. *Thrombosis Research* 125, Supplement 2, S84-S88.
- Chernitskii, E.A., Slobozhanina, E.I., Fedorovich, I.E., Novitskaia, G.P., 1994. [Vesiculation of erythrocytes during storage and connection of it with other processes in the cell]. *Biofizika* 39, 357-361.
- Christel, S., Little, C., 1984. Morphological changes during heating of erythrocytes from stored human blood. *Journal of Thermal Biology* 9, 221-228.
- Crandall, C.G., Gonzalez-Alonso, J., 2010. Cardiovascular function in the heat-stressed human. *Acta Physiol.* 199, 407-423.
- Derelanko, M.J., 1987. Determination of erythrocyte life span in F-344, Wistar, and Sprague-Dawley rats

- using a modification of the [3H]diisopropylfluorophosphate ([3H]DFP) method. *Fundamental and Applied Toxicology* 9, 271-276.
- Dey-Hazra, E., Hertel, B., Kirsch, T., Woywodt, A., Lovric, S., Haller, H., Haubitz, M., Erdbruegger, U., 2010. Detection of circulating microparticles by flow cytometry: influence of centrifugation, filtration of buffer, and freezing. *Vascular health and risk management* 6, 1125-1133.
- Dragan, A.I., Klass, J., Read, C., Churchill, M.E., Crane-Robinson, C., Privalov, P.L., 2003. DNA binding of a non-sequence-specific HMG-D protein is entropy driven with a substantial non-electrostatic contribution. *J Mol Biol* 331, 795-813.
- Dumaswala, U.J., Greenwalt, T.J., 1984. Human erythrocytes shed exocytic vesicles in vivo. *Transfusion* 24, 490-492.
- El-Sayed, M.S., Ali, N., Ali, Z.E.-S., 2005. Haemorheology in Exercise and Training. *Sports Medicine* 35, 649-670.
- Evans, E., Fung, Y.C., 1972. Improved measurements of the erythrocyte geometry. *Microvasc Res* 4, 335-347.
- Eyring, H., Lin, S.H., Lin, S.M., 1980. *Basic chemical kinetics*. John Wiley & Sons, New York.
- Foller, M., Braun, M., Qadri, S.M., Lang, E., Mahmud, H., Lang, F., 2010. Temperature sensitivity of suicidal erythrocyte death. *Eur J Clin Invest* 40, 534-540.
- Föller, M., Huber, S.M., Lang, F., 2008. Erythrocyte programmed cell death. *IUBMB Life* 60, 661-668.
- Foster, B., 2004. Focus on microscopy: a technique for imaging live cell interactions and mechanisms. *American Laboratory* 11, 21-27.
- Gallin, J.I., 1980. Degranulating stimuli decrease the negative surface charge and increase the adhesiveness of human neutrophils. *J Clin Invest* 65, 298-306.
- Gedde, M.M., Huestis, W.H., 1997. Membrane potential and human erythrocyte shape. *Biophys J* 72, 1220-1233.
- Gershfeld, N.L., Murayama, M., 1988. Thermal instability of red blood cell membrane bilayers: Temperature dependence of hemolysis. *Journal of Membrane Biology* 101, 67-72.
- Ghashghaieinia, M., Cluitmans, J.C.A., Akel, A., Dreischer, P., Toulany, M., Koberle, M., Skabytska, Y., Saki, M., Biedermann, T., Duszenko, M., Lang, F., Wieder, T., Bosman, G., 2012. The impact of erythrocyte age on eryptosis. *British Journal of Haematology* 157, 606-614.
- Glaser, R., 1979. The shape of red blood cells as a function of membrane potential and temperature. *The Journal of membrane biology* 51, 217-228.
- Glaser, R., Donath, J., 1992. Temperature and transmembrane potential dependence of shape transformations of human erythrocytes. *Journal of Electroanalytical Chemistry* 342, 429-440.
- Good, W., 1967. A Biological Example of the Compensation Law. *Nature* 214, 1250-1252.
- Greenleaf, J.E., 1979. Hyperthermia and exercise. *Int Rev Physiol* 20, 157-208.
- Greenwalt, T.J., 2006. The how and why of exocytic vesicles. *Transfusion* 46, 143-152.
- Ham, T.H., Shen, S.C., Fleming, E.M., Castle, W.B., 1948. Studies on the destruction of red blood cells. iv: thermal injury : action of heat in causing increased spheroidicity, osmotic and mechanical fragilities and hemolysis of erythrocytes; observations on the mechanisms of destruction of such erythrocytes in dogs and in a patient with a fatal thermal burn. *Blood* 3, 373-403.
- Henszen, M.M., Weske, M., Schwarz, S., Haest, C.W., Deuticke, B., 1997. Electric field pulses induce reversible shape transformation of human erythrocytes. *Molecular membrane biology* 14, 195-204.
- Hind, E., Heugh, S., Ansa-Addo, E.A., Antwi-Baffour, S., Lange, S., Inal, J., 2010. Red cell PMVs, plasma membrane-derived vesicles calling out for standards. *Biochemical and Biophysical Research Communications* 399, 465-469.
- Huang, Y.-X., Wu, Z.-J., Mehrishi, J., Huang, B.-T., Chen, X.-Y., Zheng, X.-J., Liu, W.-J., Luo, M., 2011. Human red blood cell aging: correlative changes in surface charge and cell properties. *Journal of Cellular and Molecular Medicine* 15, 2634-2642.
- Huica, R., Huica, S., Moldoveanu, E., 2011. Flow cytometric assessment of circulating microparticles - towards a more objective analysis. *Romanian Biotechnological Letters* 16, 6271-6277.
- Ivanov, I.T., 2007. Allometric dependence of the life span of mammal erythrocytes on thermal stability and sphingomyelin content of plasma membranes. *Comp Biochem Physiol A Mol Integr Physiol* 147, 876-884.
- Ivanov, I.T., Brähler, M., Georgieva, R., Bäumlner, H., 2007. Role of membrane proteins in thermal damage and necrosis of red blood cells. *Thermochimica Acta* 456, 7-12.
- Ives, D.J.G., Marsden, P.D., 1965. Ionisation functions of di-isopropylcyanoacetic acid in relation to hydration equilibria and compensation law. *Journal of the Chemical Society*, 649-676.
- Jayachandran, M., Litwiller, R.D., Owen, W.G., Heit, J.A., Behrenbeck, T., Mulvagh, S.L., Araoz, P.A., Budoff, M.J., Harman, S.M., Miller, V.M., 2008. Characterization of blood borne microparticles as markers of premature coronary calcification in

- newly menopausal women. *American Journal of Physiology - Heart and Circulatory Physiology* 295, H931-H938.
- Jun, C., Lenaghan, S.C., Mingjun, Z., 2012. Analysis of dynamics and planar motion strategies of a swimming microorganism — *Giardia lamblia*, *Robotics and Automation (ICRA), 2012 IEEE International Conference on*, pp. 4204-4209.
- Kethley, T.W., Cown, W.B., Fincher, E.L., 1963. Adequate expression for average particle size of microbiological aerosols. *Applied microbiology* 11, 188-189.
- Kozlowski, S., Brzezinska, Z., Kruk, B., Kaciuba-Uscilko, H., Greenleaf, J.E., Nazar, K., 1985. Exercise hyperthermia as a factor limiting physical performance: temperature effect on muscle metabolism. *Journal of Applied Physiology* 59, 766-773.
- Lang, F., Gulbins, E., Lang, P.A., Zappulla, D., Foller, M., 2010. Ceramide in suicidal death of erythrocytes. *Cell Physiol Biochem* 26, 21-28.
- Lang, F., Qadri, S.M., 2012. Mechanisms and significance of eryptosis, the suicidal death of erythrocytes. *Blood Purif* 33, 125-130.
- Lee, H.B., Blaufox, M.D., 1985. Blood volume in the rat. *Journal of nuclear medicine : official publication, Society of Nuclear Medicine* 26, 72-76.
- Leffler, J.E., 1955. The enthalpy-entropy relationship and its implications for organic chemistry. *The Journal of Organic Chemistry* 20, 1202-1231.
- Leon, L.R., Helwig, B.G., 2010. Heat stroke: Role of the systemic inflammatory response. *Journal of Applied Physiology* 109, 1980-1988.
- Leonards, K.S., Ohki, S., 1983. Isolation and characterization of large (0.5 - 1.0 micron) cytoskeleton-free vesicles from human and rabbit erythrocytes. *Biochim Biophys Acta* 728, 383-393.
- Leung, D.H., Bergman, R.G., Raymond, K.N., 2008. Enthalpy-Entropy Compensation Reveals Solvent Reorganization as a Driving Force for Supramolecular Encapsulation in Water. *Journal of the American Chemical Society* 130, 2798-2805.
- Lim, D.H., Jang, J., Kim, S., Kang, T., Lee, K., Choi, I.H., 2012. The effects of sub-lethal concentrations of silver nanoparticles on inflammatory and stress genes in human macrophages using cDNA microarray analysis. *Biomaterials* 33, 4690-4699.
- Loebl, E.C., Baxter, C.R., Curreri, P.W., 1973. The mechanism of erythrocyte destruction in the early post-burn period. *Ann Surg* 178, 681-686.
- Longster, G.H., Buckley, T., Sikorski, J., Derrick Tovey, L.A., 1972. Scanning electron microscope studies of red cell morphology. Changes occurring in red cell shape during storage and post transfusion. *Vox Sang* 22, 161-170.
- Lutz, H., Liu, S., Palek, J., 1977. Release of spectrin-free vesicles from human erythrocytes during ATP depletion: I. characterization of spectrin-free vesicles. *The Journal of Cell Biology* 73, 548-560.
- Mashaghi, A., Partovi-Azar, P., Jadidi, T., Nafari, N., Maass, P., Tabar, M.R., Bonn, M., Bakker, H.J., 2012. Hydration strongly affects the molecular and electronic structure of membrane phospholipids. *The Journal of chemical physics* 136, 114709.
- Morrison, S., Sleivert, G.G., Cheung, S.S., 2004. Passive hyperthermia reduces voluntary activation and isometric force production. *European Journal of Applied Physiology* 91, 729-736.
- Muller, P., Herrmann, A., Glaser, R., 1986. Further evidence for a membrane potential-dependent shape transformation of the human erythrocyte membrane. *Bioscience reports* 6, 999-1006.
- Nybo, L., Jensen, T., Nielsen, B., Gonzalez-Alonso, J., 2001. Effects of marked hyperthermia with and without dehydration on Vo(2) kinetics during intense exercise. *Journal of Applied Physiology* 90, 1057-1064.
- Nybo, L., Moller, K., Volianitis, S., Nielsen, B., Secher, N.H., 2002. Effects of hyperthermia on cerebral blood flow and metabolism during prolonged exercise in humans. *Journal of Applied Physiology* 93, 58-64.
- Nybo, L., Nielsen, B., 2001a. Hyperthermia and central fatigue during prolonged exercise in humans. *Journal of Applied Physiology* 91, 1055-1060.
- Nybo, L., Nielsen, B., 2001b. Middle cerebral artery blood velocity is reduced with hyperthermia during prolonged exercise in humans. *Journal of Physiology-London* 534, 279-286.
- Oglicka, K., Sanborn, J., Parikh, A.N., Kraut, R.S., 2012. Osmotic gradients induce bio-reminiscent morphological transformations in giant unilamellar vesicles. *Frontiers in physiology* 3, 120.
- Ogura, Y., Naito, H., Akin, S., Ichinoseki-Sekine, N., Kurosaka, M., Kakigi, R., Sugiura, T., Powers, S.K., Katamoto, S., Demirel, H.A., 2008. Elevation of body temperature is an essential factor for exercise-induced extracellular heat shock protein 72 level in rat plasma. *American Journal of Physiology - Regulatory, Integrative and Comparative Physiology* 294, R1600-R1607.
- Orozco, A.F., Lewis, D.E., 2010. Flow Cytometric Analysis of Circulating Microparticles in Plasma. *Cytometry Part A* 77A, 502-514.
- Parrott, R.F., Lloyd, D.M., Brown, D., 1999. Transport stress and exercise hyperthermia recorded in sheep by radiotelemetry. *Animal Welfare* 8, 27-34.
- Periard, J.D., Caillaud, C., Thompson, M.W., 2011. Central and Peripheral Fatigue during Passive and Exercise-Induced Hyperthermia. *Medicine and Science in Sports and Exercise* 43, 1657-1665.

- Periard, J.D., Ruell, P., Caillaud, C., Thompson, M.W., 2012. Plasma Hsp72 (HSPA1A) and Hsp27 (HSPB1) expression under heat stress: influence of exercise intensity. *Cell Stress Chaperones*.
- Przybylska, M., Bryszewska, M., K dziora, J., 2000. Thermosensitivity of red blood cells from Down's syndrome individuals. *Bioelectrochemistry* 52, 239-249.
- Rahimi, M., Kilaru, S., Sleiman, G.E., Saleh, A., Rudkevich, D., Nguyen, K., 2008. Synthesis and Characterization of Thermo-Sensitive Nanoparticles for Drug Delivery Applications. *Journal of biomedical nanotechnology* 4, 482-490.
- Repin, N.V., Bobrova, E.N., Repina, S.V., 2008. Thermally induced transformation of mammalian red blood cells during hyperthermia. *Bioelectrochemistry* 73, 101-105.
- Richards, R.S., Wang, L., Jelinek, H., 2007. Erythrocyte oxidative damage in chronic fatigue syndrome. *Arch Med Res* 38, 94-98.
- Richardson, T.M., 1988. Test slides: Diatoms to divisions-What are you looking at? *Proc Roy Microsc Soc* 22, 3-9.
- Roos, M.A., Gennero, L., Denysenko, T., Reguzzi, S., Cavallo, G., Pescarmona, G.P., Ponzetto, A., 2010. Microparticles in physiological and in pathological conditions. *Cell Biochemistry and Function* 28, 539-548.
- Rous, P., 1923. Destruction of the red blood corpuscles in health and disease. *Physiol Rev* 3, 75-106.
- Rous, P., Robertson, O.H., 1917. The normal fate of erythrocytes : i. the findings in healthy animals. *J Exp Med* 25, 651-663.
- Rubin, O., Crettaz, D., Canellini, G., Tissot, J.D., Lion, N., 2008. Microparticles in stored red blood cells: an approach using flow cytometry and proteomic tools. *Vox Sanguinis* 95, 288-297.
- Rumsby, M.G., Trotter, J., Allan, D., Michell, R.H., 1977. Recovery of membrane micro-vesicles from human erythrocytes stored for transfusion: a mechanism for the erythrocyte discocyte-to-spherocyte shape transformation. *Biochemical Society transactions* 5, 126-128.
- Samoylov, A.M., Samoylova, T.I., Pustovyy, O.M., Samoylov, A.A., Toivio-Kinnucan, M.A., Morrison, N.E., Globa, L.P., Gale, W.F., Vodyanoy, V., 2005. Novel metal clusters isolated from blood are lethal to cancer cells. *Cells Tissues Organs* 179, 115-124.
- Sawka, M.N., Wenger, C.B., 1988. Physiological Responses to Acute Exercise-Heat Stress <http://www.dtic.mil/cgi-bin/GetTRDoc?AD=ADA192606>. U.S. Army Rsch Inst of Env Med, Natick, MA.
- Schultze, M., 1865. Ein heizbarer objectisch und seine Verwendung bei Untersuchung des Blutes. *Arch. Mikrosk. Anat., Berl.* 1, 1-42.
- Segel, I.H., 1976. *Biochemical calculations.*, 2d ed. ed. John Wiley & Sons, New-York.
- Sharp, K., 2001. Entropy-enthalpy compensation: Fact or artifact? *Protein Science* 10, 661-667.
- Shet, A.S., Aras, O., Gupta, K., Hass, M.J., Rausch, D.J., Saba, N., Koopmeiners, L., Key, N.S., Hebbel, R.P., 2003. Sick blood contains tissue factor-positive microparticles derived from endothelial cells and monocytes. *Blood* 102, 2678-2683.
- Shiekh, F.A., Charlesworth, J.E., Kim, S.H., Hunter, L.W., Jayachandran, M., Miller, V.M., Lieske, J.C., 2010. Proteomic evaluation of biological nanoparticles isolated from human kidney stones and calcified arteries. *Acta Biomater* 6, 4065-4072.
- Tomlinson, E., 1983. Enthalpy entropy compensation analysis of pharmaceutical, biochemical and biological-systems. *Int J Pharm* 13, 115-144.
- Vainrub, A., O. Pustovyy, O., Vodyanoy, V., 2006. Resolution of 90 nm ($\lambda/5$) in an optical transmission microscope with an annular condenser. *Optics letters* 31, 2855-2857.
- VanWijk, M.J., VanBavel, E., Sturk, A., Nieuwland, R., 2003. Microparticles in cardiovascular diseases. *Cardiovascular Research* 59, 277-287.
- Vianna, D.M.L., Carrive, P., 2005. Changes in cutaneous and body temperature during and after conditioned fear to context in the rat. *European Journal of Neuroscience* 21, 2505-2512.
- Vittori, D., Vota, D., Nesse, A., 2012. Erythrocyte: Programmed Cell Death, in: Silverberg, D. (Ed.), *Anemia*. InTech.
- Vodyanoy, V., 2005. High resolution light microscopy of live cells. *Microscopy Today* May, 26-28.
- Vodyanoy, V., Pustovyy, O., Vainrub, A., 2007. High-resolution light microscopy of nanoforms, 669413-12, 1 ed. SPIE, San Diego, CA, USA, pp. 669413-669412.
- Vtiurin, B.V., Kaem, R.I., Chervonskaia, N.V., 1987. [Ultrastructural changes in erythrocytes and thrombocytes in patients with severe thermal burns of the skin in the burn shock period]. *Biull Eksp Biol Med* 104, 362-366.
- Wagner, G.M., Chiu, D.T., Yee, M.C., Lubin, B.H., 1986. Red cell vesiculation--a common membrane physiologic event. *J Lab Clin Med* 108, 315-324.
- Walsh, N.P., Whitham, M., 2006. Exercising in environmental extremes - A greater threat to immune function? *Sports Medicine* 36, 941-976.
- Weinkauff, H., Brehm-Stecher, B.F., 2009. Enhanced dark field microscopy for rapid artifact-free detection of nanoparticle binding to *Candida albicans* cells and hyphae. *Biotechnol J* 4, 871-879.
- Werre, J.M., Willekens, F.L., Bosch, F.H., de Haans, L.D., van der Vegt, S.G., van den Bos, A.G., Bosman, G.J., 2004. The red cell revisited--matters

- of life and death. *Cell Mol Biol (Noisy-le-grand)* 50, 139-145.
- White, M.D., Cabanac, M., 1996. Exercise hyperpnea and hyperthermia in humans. *Journal of Applied Physiology* 81, 1249-1254.
- Whitham, M., Laing, S.J., Jackson, A., Maassen, N., Walsh, N.P., 2007. Effect of exercise with and without a thermal clamp on the plasma heat shock protein 72 response. *Journal of Applied Physiology* 103, 1251-1256.
- Wikipedia, 2012a. Geometric standard deviation http://en.wikipedia.org/wiki/Geometric_standard_deviation.
- Wikipedia, 2012b. Red blood cell http://en.wikipedia.org/wiki/Red_blood_cells.
- Willekens, F.L., Bosch, F.H., Roerdinkholder-Stoelwinder, B., Groenen-Dopp, Y.A., Werre, J.M., 1997. Quantification of loss of haemoglobin components from the circulating red blood cell in vivo. *Eur J Haematol* 58, 246-250.
- Willekens, F.L., Roerdinkholder-Stoelwinder, B., Groenen-Dopp, Y.A., Bos, H.J., Bosman, G.J., van den Bos, A.G., Verkleij, A.J., Werre, J.M., 2003. Hemoglobin loss from erythrocytes in vivo results from spleen-facilitated vesiculation. *Blood* 101, 747-751.
- Willekens, F.L., Werre, J.M., Groenen-Dopp, Y.A., Roerdinkholder-Stoelwinder, B., de Pauw, B., Bosman, G.J., 2008. Erythrocyte vesiculation: a self-protective mechanism? *Br J Haematol* 141, 549-556.
- Willekens, F.L., Werre, J.M., Kruijt, J.K., Roerdinkholder-Stoelwinder, B., Groenen-Dopp, Y.A., van den Bos, A.G., Bosman, G.J., van Berkel, T.J., 2005. Liver Kupffer cells rapidly remove red blood cell-derived vesicles from the circulation by scavenger receptors. *Blood* 105, 2141-2145.
- Willekens, F.L.A., 2010. Erythrocyte vesiculation a survival strategy, Laboratory of Medical Immunology. Radboud Universiteit, Nijmegen, p. 189.
- Yeagle, P.L., 1989. Lipid regulation of cell membrane structure and function. *The FASEB Journal* 3, 1833-1842.